Occurrence and genetic implications of hyalophane in manganese-rich iron-formation, Cuyuna Iron Range, Minnesota, USA

PETER L. MCSWIGGEN, G. B. MOREY AND JANE M. CLELAND

Minnesota Geological Survey, 2642 University Avenue, St. Paul, Minnesota 55114, USA

Abstract

The recent discovery of hyalophane [$(K,Ba)Al_{1-2}Si_{3-2}O_8$] on the North range segment of the Early Proterozoic Cuyuna Iron Range of east-central Minnesota has shed new light on the depositional environment of these rocks. This Ba-feldspar occurs in a 10 m thick interval within the main iron-formation and typically contains between 8 and 26 mol.% celsian ($BaAl_2Si_2O_8$). Its occurrence in several textural settings suggests that barium was being deposited at various stages in the paragenetic history of the iron-formation. Some of the hyalophane grains occur as the cores of micronodules, which are structurally similar to oolites or oncolites, but mineralogically are very complex. The hyalophane also occurs as rims on core grains of diverse mineral composition and as discrete phases in late crosscutting veins.

Hyalophane, like other Ba-silicates, has a very restricted paragenesis. They are associated typically either with sedimentary manganese and ferromanganese deposits, or with Cu-Pb-Zn-Ba deposits. The presence of hyalophane in the Early Proterozoic manganiferous iron ores of east-central Minnesota casts doubt on the historic interpretation of these deposits as typical Superior-type sedimentary iron-formations and instead supports the view that these deposits, at least in part, consist of chemical sediments from a hydrothermal fumarolic system. The suggested involvement of a hydrothermal system is also supported by the occurrence of aegirine within the hyalophane-rich layer, and the occurrence of tourmalinites and Sr-rich baryte veins elsewhere in the Cuyuna North range.

KEYWORDS: hyalophane, Ba-feldspar, iron-formation, manganese deposits, hydrothermal activity, Cuyuna Iron Range, Minnesota.

Introduction

OUR recent discovery of hyalophane in the manganiferous iron ores of the Early Proterozoic Cuyuna Iron Range of east-central Minnesota has contributed to a re-evaluation of the depositional history of these rocks. The Cuyuna Iron Range produced more than 100 million tons of ore between 1904 and 1984, much of it containing between 5 and 15% manganese. Most of that production was from the Trommald Formation of the North Range Group, which, historically was considered to be a variant of the classic Lake Superior-type iron-formation as defined by Gross (1973). Such iron-formations are believed to have formed where iron- and silica-rich, bottom waters were brought up onto a stable continental shelf, causing iron oxides and carbonates to precipitate as primary mineral phases (e.g. Morey, 1983*a*).

As part of a larger study to evaluate the suitability of the Trommald Formation for the *in situ* extraction of manganese, we identified a number of minerals that are not consistent with a simple sedimentary origin. These include hyalophane, aegirine, rhodonite, rhodochrosite, and vein baryte, as well as stratigraphic intervals that contain appreciable tourmalinite (Cleland *et al.*, 1992; McSwiggen *et al.*, 1992). Of the various minerals recognized, hyalophane is of particular interest. It has a very restricted paragenesis and is typically found associated with manganese deposits (Deer *et al.*, 1975). Examples include the

Mineralogical Magazine, September 1994, Vol. 58, pp. 387–399

manganese deposits or manganiferous iron ores of Otjosondu, Namibia (Viswanathan and Kielhorn, 1983), Benallt mine, near Rhiw, Caernarvonshire, Wales (Spencer, 1942; Smith *et al.*, 1949), Andros Island, Greece (Reinecke, 1982), and Långban and Lillsjön, Sweden (Lundström and Wadsten, 1979; Boström *et al.*, 1979). In Japan, the Ba-feldspars celsian and hyalophane occur in many of the bedded manganese ore deposits including those from the Nodatamagawa, Kaso, Kaminagano, Shiromaru, Hamayokogawa and Taguchi mines, and those that occur in the Iwate, Tochigi, Toko, Nagano, Aichi, Hokkejino and Kyoto Prefectures (Nakano, 1979; Matsubara, 1985; Kato *et al.*, 1987).

Ba-feldspars and related barium silicates also occur associated with base metal mineralization or strata-bound baryte deposits such as those at Broken Hill, New South Wales, Australia (Segnit, 1946), the Kipushi deposit, Shaba, Zaire (Chabu and Boulègue, 1992), Cosmos Hills, Brooks Range, Alaska (Runnells, 1964), central North Greenland (Jakobsen, 1990), the Aberfeldy and Loch Lyon districts, Scotland (Fortey and Beddoe-Stephens, 1982; Coats *et al.*, 1984; Russell *et al.*, 1984), and near Braemar, Scotland (Fortey *et al.*, 1993). These barium silicate phases are also known from gold deposits such as those at Hemlo, Ontario, Canada (Pan and Fleet, 1991). Common to these different deposits is their relation to hydrothermal processes. Most are believed to be the result of volcanic exhalative activity.

Geological setting

The Cuyuna Iron Range of east-central Minnesota (Fig. 1) was discovered in 1904 and became a major mining district of iron and ferromanganese ore. It has been divided, historically, into three entities, the Emily district, the North range and the South range. The North and South ranges are part of a fold-and-thrust belt which underwent multiple deformation and metamorphism during the Penokean orogeny, at around 1870–1850 Ma (Southwick *et al.*, 1988). Mineral assemblages and carbonate geothermometry suggest that metamorphism reached upper greenschist facies. The Emily district is part of a foredeep basin that unconformably overlies the fold-and-thrust belt (Southwick *et al.*, 1988). This stratigraphic configuration is considerably different from that compiled from the older literature (Morey and Van Schmus, 1988), which assumed that the various units of iron-rich strata of the Cuyuna range were correlative, and that these strata were

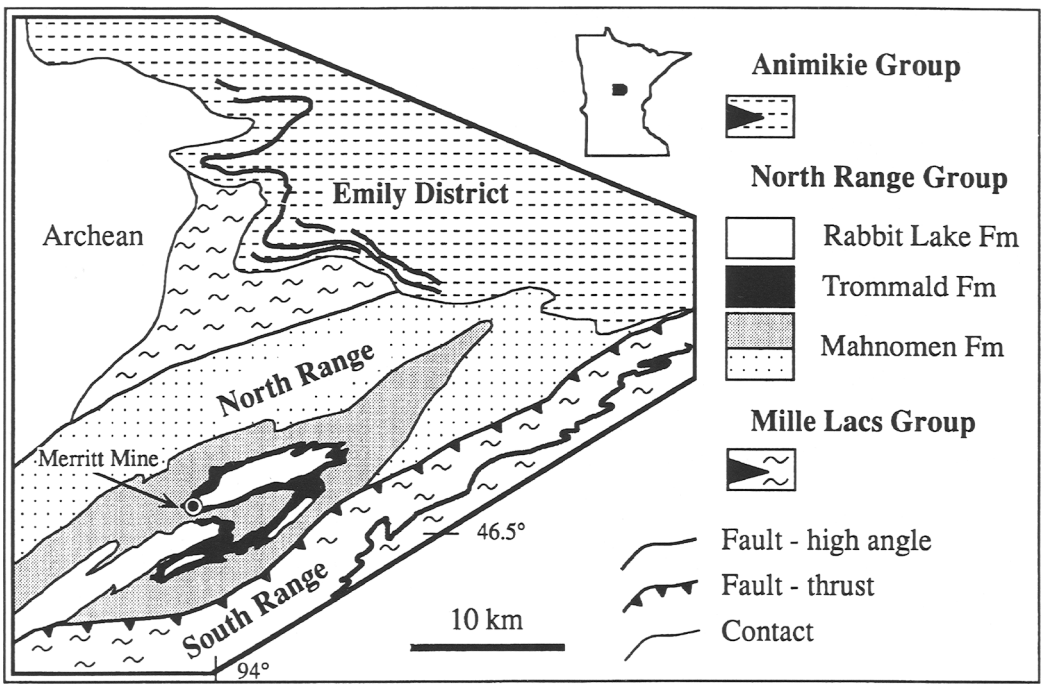

FIG. 1. General geology of the Cuyuna Iron Range (after Southwick *et al.*, 1988).

also correlative with the classic Lake Superior-type iron-formation of the Mesabi range to the northeast. The more recent structural interpretation for east-central Minnesota places the bulk of the Cuyuna range (the North and South ranges) stratigraphically beneath the Mesabi range. The bulk of the Cuyuna range is now considered to be part of a group of rocks believed to have been deposited during the early rifting stage of what became the Penokean orogen. A more detailed discussion of the general geology of east-central Minnesota and the Cuyuna range can be found in Schmidt (1963), Marsden (1972), Morey (1983*b*), Southwick *et al.* (1988), Southwick and Morey (1991), and Morey and Southwick (1993).

This study evolved from a re-investigation of core drilled at the Merritt Mine property on the Cuyuna North range (Grout and Wolff, 1955) (Fig. 1). On the North range, there are three main rock units, the Mahnomen, Trommald, and Rabbit Lake Formations (Fig. 2). The Mahnomen Formation consists of metamorphosed argillite, siltstone, and quartzose sandstone, with lesser amounts of interlayered ferruginous argillite, lean iron-formation, and volcanic rocks (Southwick *et al.*, 1988). The Trommald Formation is the main iron-formation of the North range. It consists primarily of oxide, carbonate, and silicate iron-formation (Schmidt, 1963). The Rabbit Lake Formation is the uppermost unit of the North range. It consists of a lower member of graphitic mudstone, which is interlayered with lesser amounts of iron formation and volcanic rocks, and an upper member of slate, graphitic mudstone, greywacke and thin iron-rich units (Southwick *et al.*, 1988).

At the Merritt locality, the Trommald Formation has been divided into three units an upper member of red, thick-bedded, Mn-rich, granular, oxide (hematite) iron-formation; a middle member of black, laminated, carbonate-silicate iron-formation; and a lower member of grey, thin-bedded, carbonate-silicate iron-formation (Fig. 2). The lower two units lack significant hematite but contain locally abundant amounts of diagenetic magnetite. The magnetic expression of the magnetite can be seen on the magnetic susceptibility profile in Fig. 2. This profile also

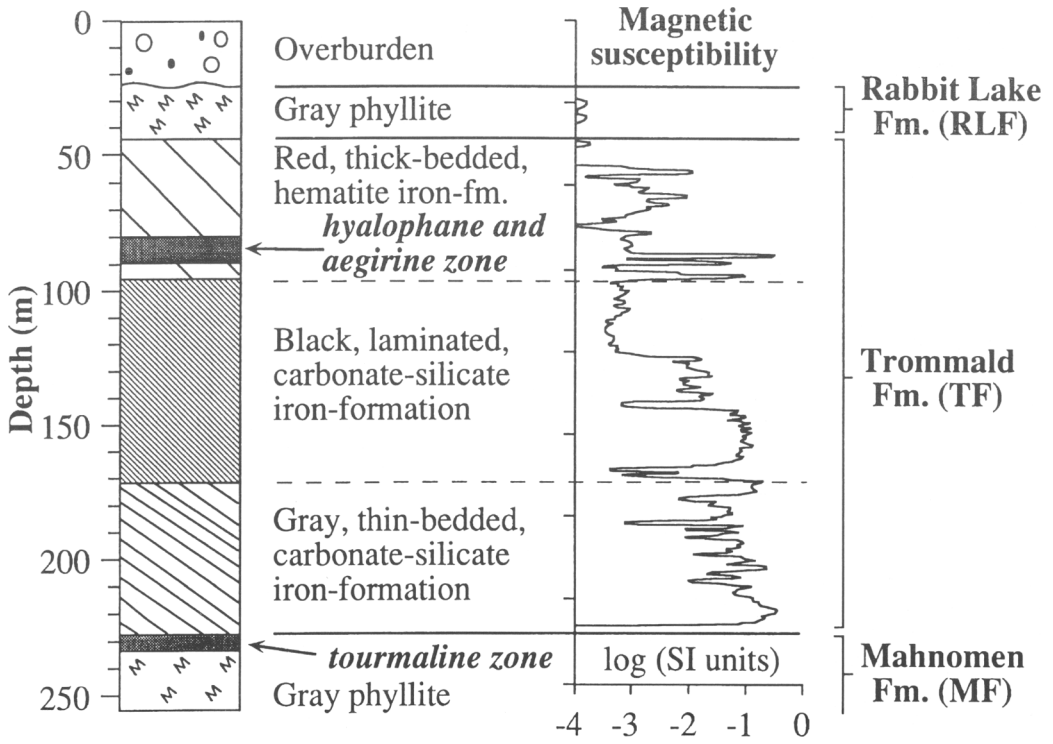

FIG. 2. Stratigraphy of the North range based on core drilled at the Merritt Mine. The hyalophane occurs in the upper member of the Trommald Formation, in this locality at depths between approximately 80 and 90 m.

shows discrete layers of magnetite-bearing strata in the upper member of the formation. At the Merritt locality, a unique characteristic of the upper member of the Trommald Formation is a hyalophane-bearing interval that is approximately 10 m thick (Fig. 2). This interval also contains abundant aegirine. Although the upper member has been interpreted in the past as typical granular, Lake Superior-type iron-formation, it is quite different. Much of the red siliceous material previously described as jasper is in fact either aegirine or rhodonite, admixed with very fine grained hematite and other phases that include magnetite, hyalophane, rhodochrosite,

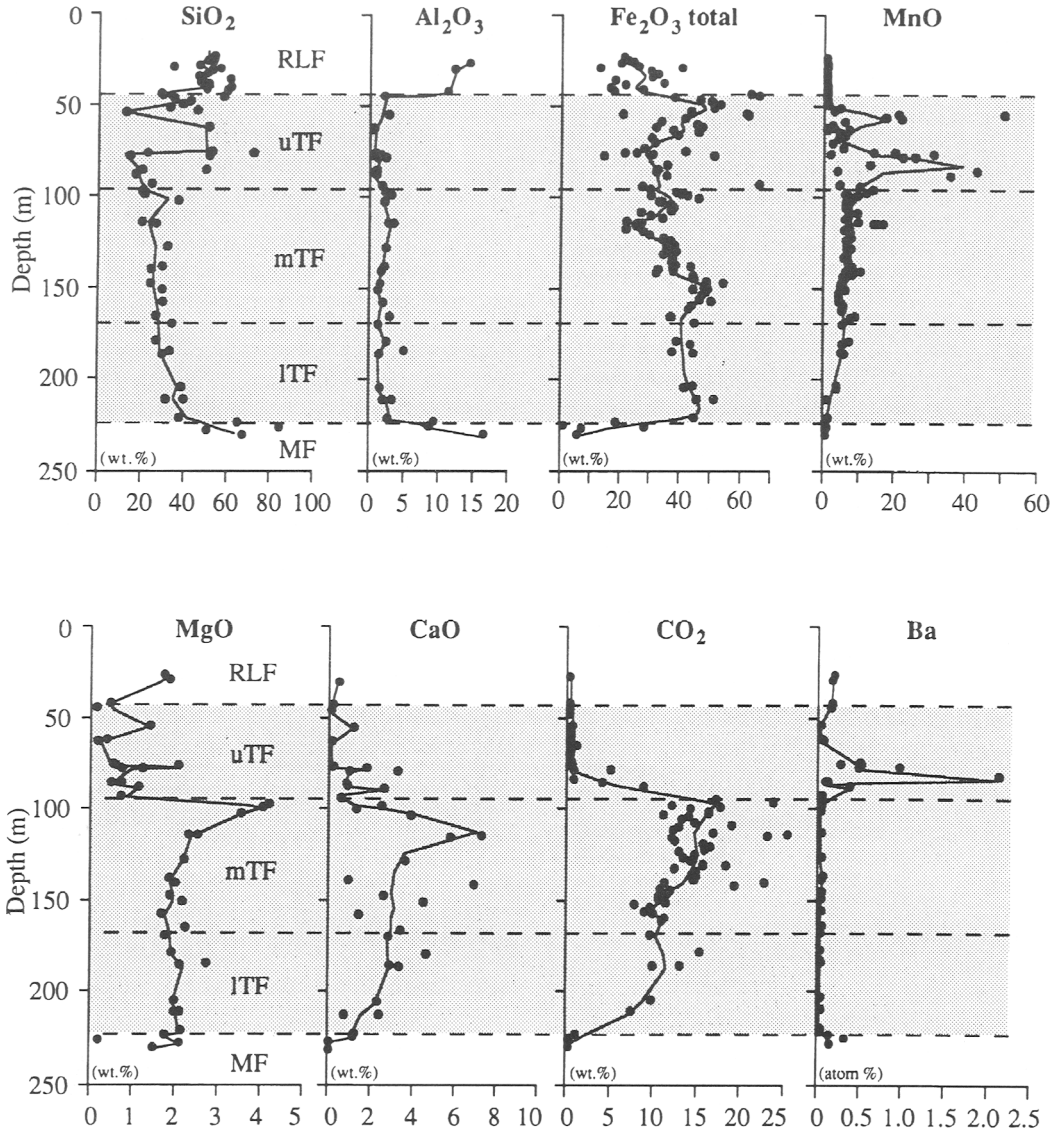

FIG. 3. Compositional profiles through the Rabbit Lake Formation (RLF), the upper (uTF), middle (mTF), and lower (lTF) members of the Trommald Formation, and the Mahnomen Formation (MF) from drill core at the Merritt Mine. Analyses are from this study and from Grout and Wolff (1955). Profiles are weighted curves, fit to the data to illustrate compositional trends.

calcite and minor amounts of stilpnomelane and magnesioriebeckite. Chert, a typical constituent of Lake Superior-type iron-formation, is conspicuously absent.

The whole-rock chemistry profiles of the Trommald Formation (Fig. 3) illustrate both the differences and similarities of its three members. Characteristic of the Trommald Formation is its very low Al_2O_3 and high total-iron content. The consistency of the iron content in the Trommald Formation is interesting considering the marked changes that occur between the upper, middle and lower members with respect to the type of iron-formation present. The change in the type of iron-formation is illustrated by the MgO, CaO and CO_2 profiles. The amount of carbonate iron-formation gradually increases from the bottom of the lower member to the top of the middle member, but then drops precipitously at the base of the upper member where the unit becomes an oxide iron-formation.

The chemistry profiles also show that the MnO content is uniformly low in the middle and lower members, but increases significantly in the upper member, although its abundance is highly variable. The lowest Mn-enriched zone of the upper member corresponds to the barium-rich horizon. Complete whole-rock analyses for major, minor, trace and rare earth elements for the hyalophane-bearing horizon are listed in Table 1.

In addition to the general characteristics of the various formations in the Cuyuna North range described above, other features also reflect on the depositional environment of these rocks. Tourmalinites and tourmaline-rich rocks have been described from localities throughout the North range (Cleland *et al.*, 1992). Typically, they occur in the Mahnomen Formation or in the

TABLE 1. Selected whole-rock analyses* of the hyalophane-bearing horizon

	1	2	3		1	2	3
SiO_2	51.0	77.1	19.9	Mo	<5	<5	<5
TiO_2	0.045	0.031	0.067	Nb	12	21	14
Al_2O_3	2.18	4.36	0.89	Ni	21	15	38
Fe_2O_3	14.1	8.77	31.57	Pb	6	<2	35
FeO	<0.1	<0.1	0.3	Rb	22	44	30
MnO	21.6	0.63	42.4	Sb	0.3	0.3	2.5
MgO	0.72	0.05	0.46	Sc	0.5	0.3	1.3
CaO	3.20	0.34	0.80	Se	<3	<3	<3
Na_2O	4.52	3.10	0.03	Sr	<10	<10	<10
K_2O	1.33	2.34	0.06	Ta	<1	<1	<1
P_2O_5	0.05	0.01	0.06	Th	<0.6	<0.5	0.9
CO_2	0.58	0.51	3.85	U	0.5	1.5	1.1
Ag	<0.5	<0.5	<0.5	V	<10	24	<10
As	42	3	270	W	<3	<3	8
Au	<5	<5	47	Y	22	<10	<10
B	29	17	34	Zn	66.8	17.6	89
Ba	9400	21100	590	Zr	<10	28	49
Be	6	15	8	La	6.5	0.7	48.5
Br	2	2	3	Ce	15	<3	49
Cd	1	<1	2	Nd	9	<5	19
Co	23	8	49	Sm	2.2	0.2	3.9
Cr	6	10	21	Eu	0.9	<0.3	1.1
Cs	2	<1	1	Th	0.7	<0.5	0.5
Cu	3.8	3.5	20.7	Yb	1.5	<0.2	2.4
Ge	<10	14	<10	Lu	0.21	<0.05	0.38
Hf	<0.6	<0.5	0.5				

1) Hyalophane- and aegirine-bearing, hematite iron formation, depth: 79.55 m.
2) Hyalophane- and aegirine-bearing vein, depth: 84.76 m.
3) Manganiferous, magnetite-bearing iron-formation, depth: 86.96 m.
* Analyses were done by XRAL Laboratories, Don Mills, Ontario. Oxides are in weight percent; elements (except Au in ppb) are in parts per million.

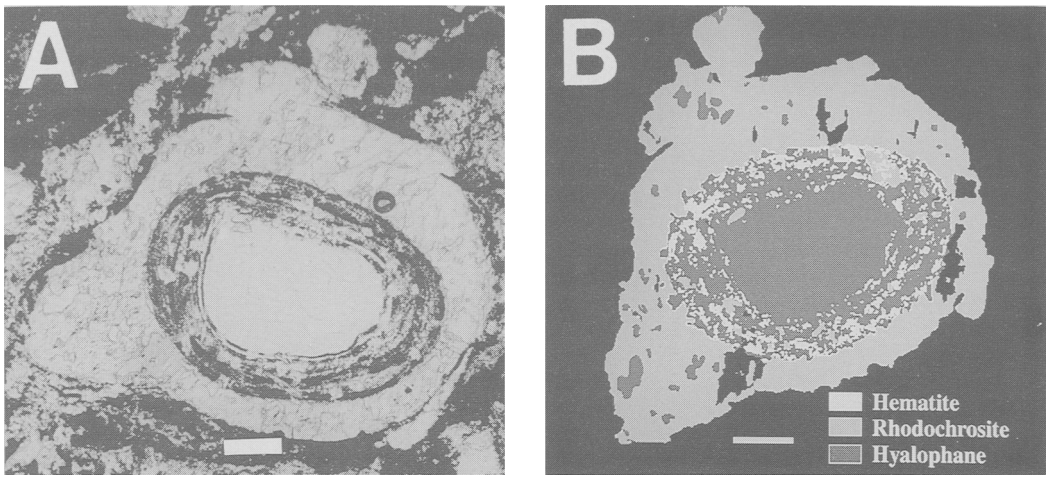

FIG. 4. Micronodule consisting of a hyalophane core grain with bands of hematite at its outer rim, which in turn is surrounded by rhodochrosite. (A) photomicrograph (transmitted light, scale bar is 100 μm) and (B) mineral map (scale bar is 100 μm).

lowermost part of the Trommald Formation, and have been found to contain as much as 35 vol. % tourmaline. Baryte veins, up to 10 cm wide, have also been found at two localities in the North range, with the baryte containing up to 6 mol. % $SrSO_4$.

Textural setting of hyalophane

The hyalophane in the Trommald Formation has a number of textural settings. In one layer, approximately 30 cm thick, hyalophane occurs as rounded clasts that form the core grains to structures (Fig. 4) that were previously described as oolites or oncolites (Grout, 1946; Grout and Wolff, 1955). However, their mineralogical attributes preclude a simple sedimentary origin. For this reason they are referred to here simply as micronodules.

Micronodules of the kind illustrated in Fig. 4 consist of several mineral phases. The core grains typically consist of hyalophane, aegirine, rhodo-

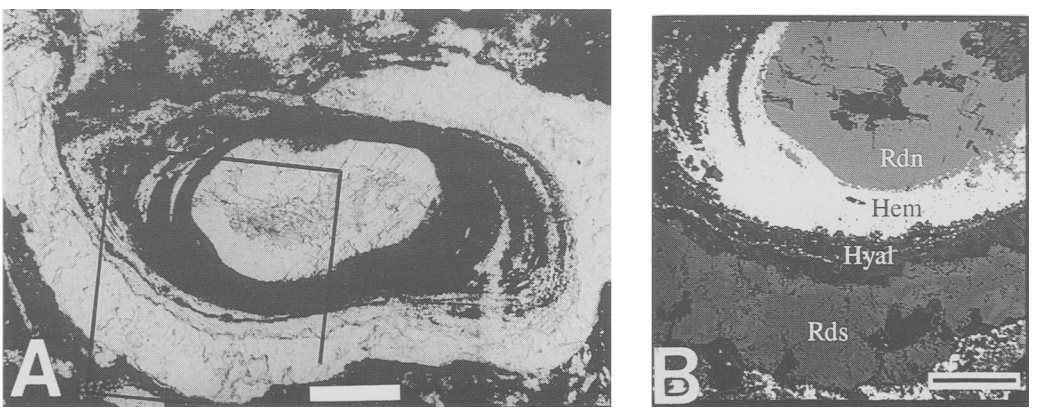

FIG. 5. Micronodule consisting of a rhodonite (Rdn) core, surrounded by hematite (Hem), hyalophane (Hyal), and finally rhodochrosite (Rds). (A) photomicrograph (transmitted light, scale bar is 100 μm) and (B) backscattered electron image (scale bar is 50 μm).

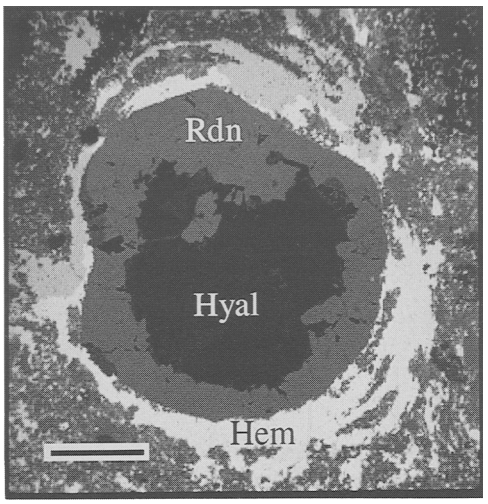

FIG. 6. Backscattered electron image of a grain consisting of a hyalophane (Hyal) core and rhodonite (Rdn) rim. The rhodonite appears to be replacing the hyalophane. Surrounding the rhodonite rim is a groundmass of hematite (Hem, white) and rhodonite (scale bar is 50 μm).

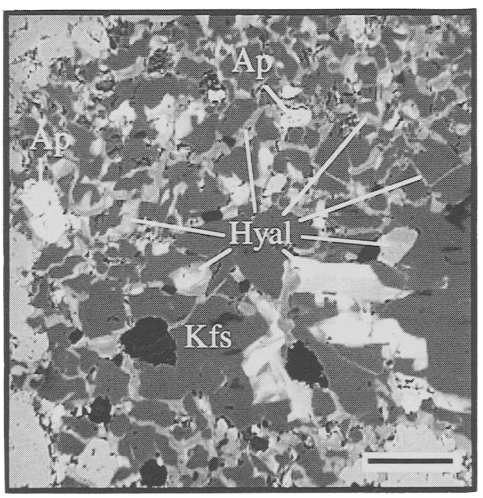

FIG. 7. Backscattered electron image of secondary hyalophane (Hyal) mineralization within a brecciated K-feldspar (Kfs) grain (see analyses 1 and 2, Table 2). Crystal also contains included grains of apatite (Ap) (scale bar is 50 μm).

nite, hematite, Mn oxide or rhodochrosite. The rims surrounding the core grains also are variable and consist of one or more of these phases. Fig. 5 illustrates one of the more elaborate examples. It consists of a core grain of rhodonite, which is successively mantled by hematite, hyalophane, and rhodochrosite.

The fine banding in the core grains of some micronodules, such as the hematite banding in Fig. 4, suggests that these are not simply detrital grains washed into the basin from the surrounding terrane, but that at least some of these core grains formed on the seafloor. Hyalophane rims in other micronodules (Fig. 5) also have an enigmatic paragenesis. They must represent a period in which barium, aluminium and silica were accumulating on a pre-existing grain or nodule, although the exact form of depositional material is not known. It may have been as a Ba-Al-Si gel, from which the silicate phase grew during diagenesis (Coats *et al.*, 1980). However, the fact that in this example (Fig. 5), the hyalophane surrounds a hematite coating and is in turn surrounded by rhodochrosite, argues that these phases or their precursors were being deposited from a very complex and changing aqueous solution.

The micronodules were undoubtedly later modified during diagenesis and metamorphism. The extent to which they have been affected by these later events appears to be variable. For example, the micronodule in Fig. 4 appears very pristine compared to that in Fig. 6, where the hyalophane has been partially replaced by rhodonite.

Hyalophane also occurs in crosscutting veins and in veins filling tension gashes. In some veins the hyalophane occurs with rhodonite; other phases that may be present include calcite, rhodochrosite, quartz and magnesioriebeckite. A second set of veins consists of hyalophane, aegirine and quartz. The occurrence of hyalophane in these veins argues that periods of barium mobility persisted through the orogenic events that affected these rocks. Hyalophane also occurs with K-feldspars, both as thin rims and as fracture filling in brecciated grains (Fig. 7). Lastly, hyalophane was found as isolated angular or euhedral grains in a groundmass of aegirine, rhodochrosite, hematite and Mn-oxide.

Hyalophane chemistry

Hyalophane occurs along the binary solid solution series between $KAlSi_3O_8$ (orthoclase) and $BaAl_2Si_2O_8$ (celsian). According to Deer *et al.* (1975), hyalophane generally contains between 5

TABLE 2. Electron-microprobe analyses of hyalophane and K-feldspar

(wt.%)	1	2	3	4	5	6	7	8	9	10	11	12
SiO_2	57.45	64.54	53.93	60.77	57.40	59.22	59.13	59.54	57.57	61.31	60.72	61.58
Al_2O_3	20.48	18.35	21.06	19.57	20.23	20.38	19.97	19.41	20.35	19.86	20.36	19.40
BaO	10.41	0.14	13.31	4.80	9.67	9.09	7.04	6.97	9.13	5.09	6.66	4.49
CaO	0.00	0.00	0.00	0.00	0.00	0.03	0.00	0.00	0.00	0.01	0.01	0.00
Na_2O	0.31	0.31	0.50	0.55	0.35	0.42	0.64	0.64	0.66	0.64	0.56	0.45
K_2O	11.46	16.48	10.66	14.09	12.29	11.04	13.11	12.81	12.18	13.78	12.02	14.37
Total	100.11	99.81	99.47	99.78	99.94	100.18	99.94	99.36	99.89	100.69	100.44	100.40
Number of ions on the basis of 8 atoms of oxygen												
Si	2.823	2.995	2.737	2.902	2.825	2.862	2.861	2.888	2.823	2.900	2.887	2.918
Al	1.186	1.004	1.260	1.101	1.174	1.161	1.140	1.110	1.177	1.107	1.141	1.084
Ba	0.200	0.003	0.265	0.090	0.186	0.172	0.133	0.132	0.175	0.094	0.124	0.083
Ca	0.000	0.000	0.000	0.000	0.000	0.002	0.000	0.000	0.000	0.000	0.001	0.000
Na	0.030	0.028	0.050	0.051	0.033	0.039	0.060	0.060	0.063	0.059	0.051	0.041
K	0.718	0.976	0.690	0.859	0.772	0.681	0.809	0.793	0.762	0.831	0.729	0.869
%Or	76	97	69	86	78	76	81	80	76	84	81	87
%Ab	3	3	5	5	3	4	6	6	6	6	6	4
%An	0	0	0	0	0	0	0	0	0	0	0	0
%Cn	21	0	26	9	19	19	13	13	18	10	14	8

1) Hyalophane vein filling in a brecciated K-feldspar grain of analysis #2, depth: 80.04 m.
2) Brecciated K-feldspar, infilled with hyalophane of analysis #1, depth: 80.04 m.
3) Hyalophane in vein with aegirine and quartz, depth: 84.76 m.
4) Host hyalophane shown in Fig. 10. Vein filling intergrown with rhodonite, depth: 84.98 m.
5) Exsolved hyalophane in contact with host material of analysis #4.
6) Hyalophane coating shown in Fig. 5, depth: 89.82 m.
7) Hyalophane core grain rimmed by rhodonite, shown in Fig. 6, depth: 89.61 m.
8) Hyalophane core grain rimmed by hematite and rhodochrosite, shown Fig. 5, depth: 89.82 m..
9) Compositionally zoned hyalophane shown in Fig. 9, analysis of BaO-rich zone, depth: 82.63 m.
10) Same hyalophane grain as in #9, but analysis is from BaO-poor zone.
11) Small hyalophane grain in a matrix of rhodochrosite and chert, depth: 82.63 m.
12) Same as analysis #11.

Electron microprobe analyses were carried out using wavelength dispersive spectrometers on a Cameca SX 50 instrument at the University of Chicago using an accelerating voltage of 15 kV, a beam current of 25 nA, and a beam diameter of approximately 5 microns. The following standards were used: anorthite (Ca, Al, Si), Asbestos microcline (K), Amelia albite (Na), and paracelsian (Ba). Counting times were 10 s for all elements except for Si and Al which had counting times of 5 s. Data reduction was done using a PAP correction routine (Pouchou and Pichoir, 1984).

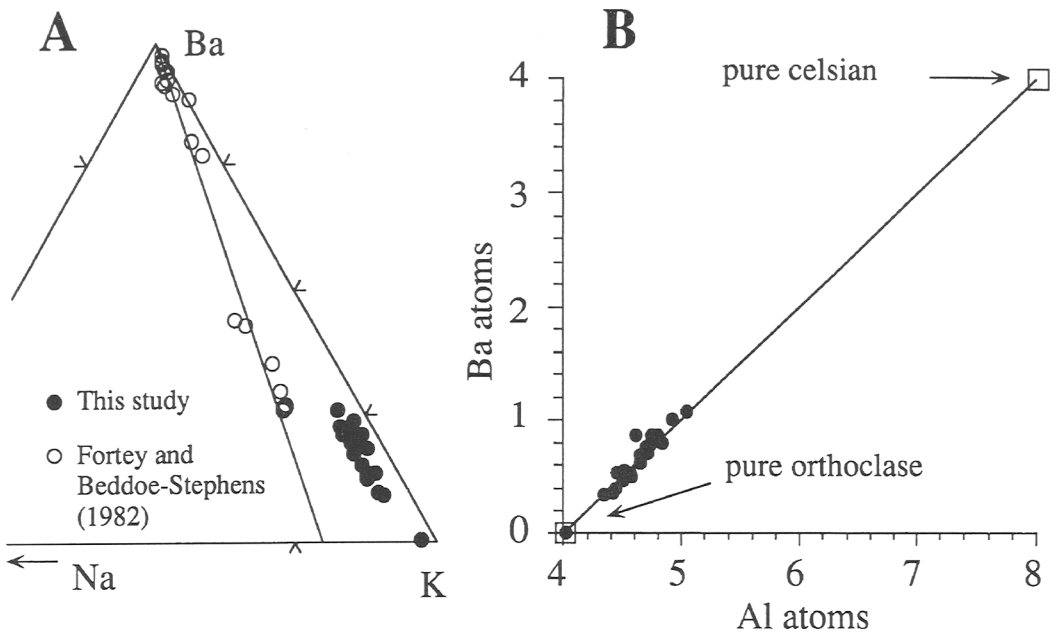

FIG. 8. Composition of hyalophane as shown on (A) a Ba-K-Na plot, and (B) a Ba-Al plot (after Fortey and Beddoe-Stephens, 1982).

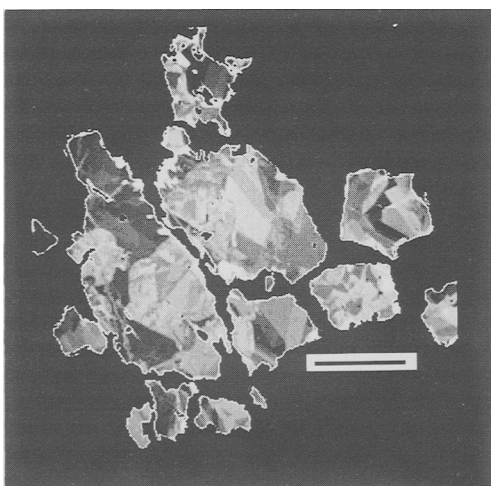

FIG. 9. Backscattered electron image showing compositional zoning in hyalophane grains. Surrounding matrix was digitally removed from image. The BaO content ranges from 5–9 wt.% (see analyses 9 and 10, Table 2). The lighter areas are higher in BaO (scale bar is 50 μm).

and 30 mol. % celsian. However, hyalophane is not restricted to this compositional range, and higher celsian contents are reported from many localities (Pan and Fleet, 1991; Chabu and Boulègue, 1992). The primary substitution is between BaAl and KSi (Gay and Roy, 1968). Gay and Roy (1968) have argued that the rarity of Ba-rich feldspar is due more to the lack of suitable conditions in nature than to any fundamental dffficulties in accommodating the Ba cation in the feldspar structure. Therefore one should regard $BaAl_2Si_2O_8$ as part of the quaternary feldspar system.

In the Trommald Formation, hyalophane contains between 8 and 26 mol.% celsian (Table 2, Fig. 8). There is no significant anorthite component, and the albite component is relatively constant at between 3 and 6 mol.%. Barium zoning is common in the larger hyalophane grains (Fig. 9), and typically is very complex. In general this type of zoning appears to be a replacement texture, and the hyalophane has simply not re-equilibrated into a single homogeneous composition.

Exsolution features that are evident in some hyalophane grains (Fig. 10) suggest that the bulk composition of those grains falls within an

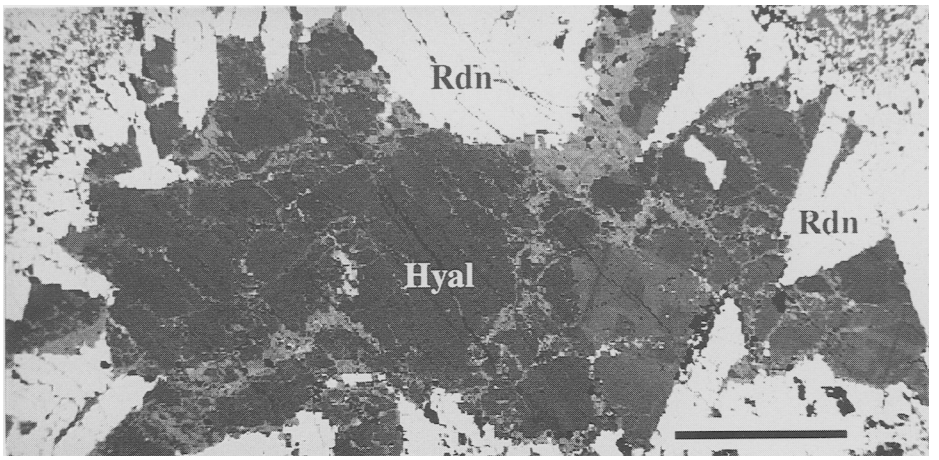

FIG. 10. Backscattered electron image of exsolution features in hyalophane (Hyal). The hyalophane is part of a vein filling that also contains rhodonite (Rdn). The lighter hyalophane lamellae have a higher BaO content (see analyses 4 and 5, Table 2, scale bar is 500 μm).

immiscible zone along the binary solid solution for the temperature at which the crystal equilibrated. In the example shown in Fig. 10, the hyalophane host grain contains an average of 9 mol.% celsian, and irregular patches and veinlets contain an average of 19 mol.% celsian (Table 2, analyses 4 and 5).

Gay and Roy (1968) speculated that a zone of immiscibility occurs between 1 and 15 mol.% percent celsian and a second zone between 65 and 80 mol.% celsian.

Three compositional discontinuities have been reported by Pan and Fleet (1991), at Cn_{15-25}, Cn_{30-40} and Cn_{47-65}. Various immiscible zones along the binary between K-feldspar and celsian have also been reported by Nakano (1979), Fortey and Beddoe-Stephens (1982), and Chabu and Bolègue (1992). However, a comparison of the various estimated positions for these miscibility gaps shows that there is considerable disagreement.

These differences may have resulted from a number of factors, including that the rocks of the various investigations equilibrated at different temperatures; that the hyalophane grains typically contained variable amounts of other components, in particular sodium; and that the hyalophane being investigated possibly had not truly equilibrated. None the less, by judicious use of natural assemblages, it should be possible to estimate the positions of various solvi along this binary. If the data are limited to low-Na_2O feldspars, it is possible to determine the position of at least the BaO-poor limb of the lowest-celsian solvus (Fig. 11). For the Cuyuna range, the best examples of coexisting hyalophane, whose textures suggest a reasonable degree of re-equilibration, are those having exsolution features. In Fig. 10, the hyalophane grain is from a secondary vein whose deformation suggests involvement in the Penokean orogeny. We have estimated metamorphic temperatures for the Cuyuna North range from coexisting kutnahorite and rhodochrosite. The position of this solvus has been experimentally determined by Goldsmith and Graf (1957). On the basis of the compositions of the two coexisting carbonates, we estimate the temperature of the regional Penokean metamorphism near the Merritt Mine at between 480° and 490°C. A temperature of 450°C was estimated for later carbonate veins. It is assumed that the hyalophane exsolution features were the result of re-equilibration within this temperature range. Hopefully, future work will allow for other limbs along the binary to be constrained in a like manner.

Discussion

Generally, hyalophane is thought to form via one of two processes, either from baryte or from an earlier Ba-silicate phase. Bjørlykke and Griffin (1973) have shown that in the Oslo region of Norway, hyalophane is pseudomorphic after baryte. It is believed that the baryte was deposited in an environment that was sufficiently oxidizing to form SO_4^{2-}. During a later diagenetic or

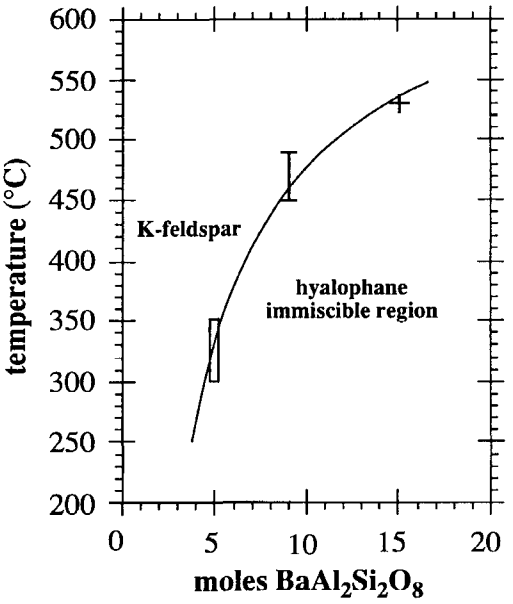

FIG. 11. Inferred relationship between celsian content of K-feldspar, coexisting with hyalophane, and temperature: data values are from this study (bar), Chabu and Boulègue (1992) (rectangle), and Pan and Fleet (1991) (cross).

metamorphic event, the baryte was redissolved as a result of a more reducing environment, and the barium was reprecipitated as hyalophane. In other localities, the hyalophane is viewed as an authigenic phase formed from what was originally a Ba-Al-Si gel (Coats *et al.*, 1980). In this model, the process by which the celsian component of hyalophane formed was multi-staged, beginning with harmotome ($BaAl_2Si_6O_{16}\cdot 6H_2O$) or an unnamed hydrous Ba-silicate ($BaAl_2Si_2O_8\cdot 4H_2O$) (Jakobsen, 1990). Following a series of essentially dehydration reactions, these phases reacted to form cymrite ($BaAl_2Si_2O_8\cdot H_2O$), and finally celsian ($BaAl_2Si_2O_8$) (Jakobsen, 1990; Matsubara, 1985; Fortey and Beddoe-Stephens, 1982).

There is no textural evidence that the hyalophane in the Cuyuna range formed as a replacement of baryte. The fine laminations of some micronodules (Fig. 4) imply that the Ba-phase did not undergo a complete cation replacement, as would be required if it was pseudomorphic after baryte. Most likely the hyalophane formed from an earlier Ba-Al-silicate phase that underwent dehydration during diagenesis or metamorphism. However, the hyalophane-bearing interval contains mineral assemblages, including hematite and aegirine, that indicate that deposition and diagenesis occurred under fairly oxidizing conditions. Therefore, if there had been sulphur available, baryte should have been able to form. The absence of baryte at this locality, or evidence that baryte was the precursor phase, may indicate an absence of sulphur in the seawater during deposition. A scarcity of sulphur in the seawater may indicate that it had been earlier removed by the precipitation of sulphides and sulphates elsewhere in the basin.

We have found that barium-rich rocks are an atypical sedimentary constituent of Lake Superior-type iron-formations. Instead the barium-bearing strata of the Cuyuna range are more akin to those associated with the bedded manganese and ferromanganese deposits and the stratabound Pb-Zn-Cu-sulphide and baryte deposits discussed above. These sulphide and sulphate deposits are generally believed to be hydrothermal in origin (Page and Watson, 1976; Coats *et al.*, 1980; Fortey and Beddoe-Stephens, 1982; Russell *et al.*, 1984; Jakobsen, 1990; Fortey *et al.*, 1993), as are many if not most of the bedded manganese and ferromanganese deposits (Matsubara, 1985). Typically, it is argued that the Ba in exhalative environments was derived from underlying oceanic basalts or barium-rich sediments by the interaction of seawater heated and circulated by nearby volcanic activity (Russell *et al.*, 1984; Matsubara, 1985; Jakobsen, 1990). In this model, heated fluids are drawn down through the underlying country rocks, leaching them of their heavy metals that include Mn, Fe, Cu, Zn and Ba. These metal-laden solutions are subsequently vented onto the seafloor where they lose their metal load.

We suggest that the hyalophane-bearing interval is evidence for the existence of this type of hydrothermal system on the North range. Other evidence for such a hydrothermal system includes the presence of aegirine in the hyalophane layer, the existence of tourmalinites at many localities along the North range, and the presence of Sr-rich baryte veins elsewhere on the North range (McSwiggen *et al.*, in press; McSwiggen *et al.*, 1992; Cleland *et al.*, 1992). Tourmalinites and Sr-rich baryte deposits are commonly associated with submarine exhalative deposits (Large, 1980; Ethier and Campbell, 1977), where B, Ba, and/or Sr-rich fluids are abundant. Aegirine can form authigenically but requires the presence of a NaCl-rich fluid. Experimental results, together with the absence of aegirine as a common mineral in hematite-bearing, sedimentary iron-formations,

indicate that the aegirine was deposited in the presence of a fluid with a greater NaCl content than normal seawater or a higher temperature (McSwiggen *et al.*, in press). Either or both of these conditions could be achieved near a fumarolic vent system.

At this time we do not know the extent to which hydrothermal activity contributed to the deposition of the Trommald Formation, but it would explain the high manganese content in portions of this unit. The existence of such a hydrothermal system also has significant implications for base-metal mineral exploration in the area. Many of the mineralogical attributes of the North range are akin to those associated with sedimentary Cu-Pb-Zn sulphide deposits elsewhere in the world (Large, 1980). Therefore it is possible that similar sulphide deposits may be found on the North range.

As mentioned above, the presence of hyalophane and the absence of baryte may indicate a lack of sulphur in the seawater during the deposition of the upper part of the Trommald Formation in this locality. However, as Russell *et al.* (1984) point out, in an oxidizing environment, the barium coming from a vent system would first precipitate as baryte, and this reaction would continue until the sulphur in the seawater was consumed. The remaining barium would then precipitate as some hydrated Ba-Al-silicate. The result is an apron or sheath of Ba-silicates around a baryte deposit, which may occur as an apron or sheath around an earlier formed Cu-Pb-Zn sulphide deposit. Therefore it is conceivable that the hyalophane described here represents the outer fringe of such a vent system on the Cuyuna North range.

Acknowledgements

This project was partially supported by the U.S. Bureau of Mines — Selective Mining in Minnesota. We would like to thank E. Grew and an anonymous reviewer, whose helpful comments and suggestions improved this manuscript, and Ian Steele, who assisted with the electron-microprobe analyses.

References

Bjørlykke, K. O., and Griffin, W. L. (1973) Barium feldspar in Ordovician sediments, Oslo region, Norway. *J. Sediment. Petrol.*, **43**, 461–5.

Boström, K., Rydell, H. and Joensuu, O. (1979) Långban — an exhalative sedimentary deposit? *Econ. Geol.*, **74**, 1002–11.

Chabu, M. and Boulègue, J. (1992) Barian feldspar and muscovite from the Kipushi Zn-Pb-Cu deposit, Shaba, Zaire. *Can. Mineral.* **30**, 1143–52.

Cleland, J. M., Morey, G. B. and McSwiggen, P. L. (1992). Occurrence of tourmaline-rich rocks in the Trommald and Mahnomen Formations of the Cuyuna range, east-central Minnesota (abstr.). *Geol. Soc. Amer. Abstr. Prog., Annual Meeting, Cincinnati*, A62.

Coats, J. S., Fortey, N. J., Gallagher, M. J. and Grout A. (1984) Stratiform barium enrichment in the Dalradian of Scotland. *Econ. Geol.*, **79**, 1585–95.

Coats, J. S., Smith, C. G., Fortey, N. J., Gallagher, M. J., May, F. and McCourt, W. J. (1980) Strata-bound barium-zinc mineralization in Dalradian schist near Aberfeldy, Scotland. *Trans. Inst. Mining Metall. (Sect. B: Appl. Earth Sci.)*, **89**, 110–22.

Deer, W. A., Howie, R. A. and Zussman, J. (1975) *An introduction to the rock forming minerals.* Longman, London, 528 pp.

Ethier, V. G. and Campbell, F. A. (1977) Tourmaline concentrations in Proterozoic sediments of the southern Cordillera of Canada and their economic significance. *Can. J. Earth Sci.*, **14**, 2348–63.

Fortey, N. J. and Beddoe-Stephens, B. (1982) Barium silicates in stratabound Ba-Zn mineralization in the Scottish Dalradian. *Mineral. Mag.*, **46**, 63–72.

Fortey, N. J., Coats, J. S., Gallagher, M. J., Smith, C. G. and Greenwood, P. G. (1993) New strata-bound barite and base metals in Middle Dalradian rocks near Braemar, northeast Scotland. *Trans. Inst. Mining Metall. (Sect. B: Appl. Earth Sci.)*, **102**, 55–64.

Gay, P., and Roy, N. N. (1968) The mineralogy of the potassium-barium feldspar series III: Subsolidus relationships. *Mineral. Mag.*, **36**, 914–32.

Goldsmith, J. R. and Graf, D. L. (1957) The system CaO–MnO–CO_2: Solution and decomposition relations. *Geochim. Cosmochim. Acta*, **11**, 310–34.

Gross, G. A. (1973) The depositional environment of principal types of Precambrian iron-formation. In *Genesis of Precambrian iron and manganese deposits.* UNESCO, *Earth Science Series*, **9**, 15–21.

Grout, F. F. (1946) Acmite occurrences on the Cuyuna range, Minnesota. *Amer. Mineral.* **31**, 125–30.

Grout, F. F. and Wolff, J. F. (1955) The geology of the Cuyuna district, Minnesota: A progress report. *Minn. Geol. Surv. Bull.*, **36**, 144 pp.

Jakobsen, U. H. (1990) A hydrated barium silicate in unmetamorphosed sedimentary rocks of central North Greenland. *Mineral. Mag.*, **54**, 81–9.

Kato, A., Matsubara, S. and Watanabe, T. (1987) Banalsite and serandite from the Shiromaru mine, Tokyo. *Bull. Natn. Sci. Mus., Tokyo, Ser. C*, **13**, 107–14.

Large, D. E. (1980) Geological parameters associated with sediment-hosted submarine exhalative Pb-Zn deposits: An empirical model for mineral exploration. *Geol, Jb.*, **40**, 59–129.

Lundström, I. and Wadsten, T. (1979) Barium feldspar from Lillsjön, southern Sweden. *Geologiska Föreningens i Stockholm Förhandlingar*, **101**, 229–32.

Marsden, R. W. (1972) Cuyuna district. In *Geology of Minnesota: A centennial volume* (P. K. Sims and G. B. Morey, eds.). *Minn. Geol. Sur.*, 227–39.

Matsubara, S. (1985) The mineralogical implication of barium and strontium silicates. *Bull. Natn. Sci. Mus., Tokyo, Ser. C*, **11**, 37–95.

McSwiggen, P. L., Morey, G. B. and Cleland, J. M. (1992) Occurrence of Ba-feldspar, acmite/aegirine, and Sr-rich barite in the Trommald iron-formation of the Cuyuna fron Range, east-central Minnesota: Implications of an hydrothermal origin (abstr.). *Geol. Soc. Amer. Abstr. Prog., Annual Meeting, Cincinnati*, A62.

McSwiggen, P. L., Morey, G. B. and Cleland, J. M. The origin of aegirine in iron formation of the Cuyuna range, east-central Minnesota. *Can. Mineral.*, (in press).

Morey, G. B. (1983*a*) Animikie basin, Lake Superior region, U.S.A., In *Iron-formation facts and problems* (A. F. Trendall and R. C. Morris, eds.). Elsevier, Amsterdam, 13–67.

Morey, G. B. (1983*b*) Lower Proterozoic stratified rocks and the Penokean orogeny in east-central Minnesota. In *Early Proterozoic Geology of the Great Lakes Region* (L. G. Medaris, Jr., ed.). *Geol. Soc. Amer. Mem.*, **160**, 97–112.

Morey, G. B. and Southwick, D. L. (1993) Stratigraphic and sedimentological factors controlling the distribution of epigenetic manganese deposits in iron-formation of the Emily District, Cuyuna Iron Range, east-central Minnesota. *Econ. Geol.*, **88**, 104–22.

Morey, G. B. and Van Schmus, W.R. (1988) Correlation of Precambrian rocks of the Lake Superior region, United States. *U.S. Geol. Surv. Prof. Paper*, **1241–F**, 31 pp.

Nakano S. (1979) Intergrowth of barium microcline, hyalophane and albite in the barium-containing alkali feldspar from the Noda-Tamagawa mine, Iwate Prefecture, Japan. *Mineral. J.*, **9**, 409–16.

Page, D. C. and Watson, M. D. (1976) The Pb-Zn deposit of the Rosh Pinah Mine, South West Africa. *Econ. Geol.*, **71**, 306–27.

Pan, Y. and Fleet, M. E. (1991) Barian feldspar and barian-chromian muscovite from the Hemlo area, Ontario. *Can. Mineral.*, **29**, 481–98.

Pouchou, J. L. and Pichoir, F. (1984) A new model for quantitative X-ray microanalysis, Part I: Application to the analyses of homogeneous samples. *Rech. Aerosp.*, **3**, 13–38.

Reinecke, T. (1982) Cymrite and celsian in manganese-rich metamorphic rocks from Andros Island/ Greece. *Contrib. Mineral. Petrol.*, **79**, 333–6.

Runnells, D. D. (1964) Cymrite in a copper deposit, Brooks Range, Alaska. *Amer. Mineral.*, **49**, 158–65.

Russell, M. J., Hall, A. J., Willan, R. C. R., Allison, I., Anderton, R. and Bowes, G. (1984) On the origin of the Aberfeldy celsian + baryte + base-metal deposits, Scotland. In *Symposium on prospecting in areas of glaciated terrain, Glasgow, Scotland* (M. J. Gallagher, ed.), 158–70.

Schmidt, R. G. (1963) Geology and ore deposits of the Cuyuna North range. *U.S. Geol. Surv. Prof. Paper*, **407**, 96 pp.

Segnit, E. R. (1946) Barium-feldspar from Broken Hill, New South Wales. *Mineral. Mag.*, **27**, 166–74.

Smith, W. C., Bannister, F. A. and Hey, M. H. (1949) Cymrite, a new barium mineral from the Benallt manganese mine, Rhiw, Carnarvonshire. *Mineral. Mag.*, **28**, 676–81.

Southwick, D. L. and Morey, G. B. (1991) Tectonic imbrication and foredeep development in the Penokean orogen, east-central Minnesota — An interpretation based on regional geophysics and the results of test-drilling. *U.S. Geol. Sur. Bull.*, **1904-C**, C1–C17.

Southwick, D. L., Morey, G. B. and McSwiggen, P. L. (1988) Geologic map (scale 1:250,000) of the Penokean orogen, central and eastern Minnesota, and accompanying text. *Minn. Geol. Surv. Rept. Inv.*, **37**, 25 pp.

Spencer, L. J. (1942) Barium-feldspars (celsian and paracelsian) from Wales. *Mineral. Mag.*, **26**, 231–45.

Viswanathan, K. and Kielhorn, H. M. (1983) Variations in the chemical compositions and lattice dimensions of (Ba,K,Na)-feldspars from Otjosondu, Namibia and their significance. *Amer. Mineral.*, **68**, 112–21.

[*Manuscript received 21 September: revised 6 January 1994*]